High performance pentacene organic field-effect transistors consisting of biocompatible PMMA/silk fibroin bilayer dielectric*

Li Hai-Qiang(李海强), Yu Jun-Sheng(于军胜)†, Huang Wei(黄 伟), Shi Wei(施 薇), and Huang Jiang(黄 江)

State Key Laboratory of Electronic Thin Films and Integrated Devices, School of Optoelectronic Information, University of Electronic Science and Technology of China, Chengdu 610054, *China*

(Received 6 July 2013; revised manuscript received 1 August 2013; published online 24 January 2014)

Pentacene organic field-effect transistors (OFETs) based on single- or double-layer biocompatible dielectrics of poly(methyl methacrylate) (PMMA) and/or silk fibroin (SF) are fabricated. Compared with those devices based on single PMMA or SF dielectric or SF/PMMA bilayer dielectric, the OFETs with biocompatible PMMA/SF bilayer dielectric exhibit optimal performance with a high field-effect mobility of 0.21 cm^2/Vs and a current on/off ratio of 1.5×10^4. By investigating the surface morphology of the pentacene active layer through atom force microscopy and analyzing the electrical properties, the performance enhancement is mainly attributed to the crystallization improvement of the pentacene and the smaller interface trap density at the dielectric/organic interface. Meanwhile, a low contact resistance also indicates that a good electrode/organic contact is formed, thereby assisting the performance improvement of the OFET.

Keywords: organic filed-effect transistors (OFETs), poly(methyl methacrylate), silk fibroin, bilayer dielectric

PACS: 85.30.Tv, 85.50.–n, 68.35.–p, 73.40.Cg **DOI:** 10.1088/1674-1056/23/3/038505

1. Introduction

Organic field-effect transistors (OFETs) have attracted considerable attention for their potential applications in low-cost electronic devices such as radio-frequency identification (RFID) tags, flexible electronic papers, and backplane circuits for active matrix displays and sensors.[1–5] By modifying the dielectric/organic or organic/electrode interfaces, the performances of OFETs have been dramatically improved.[6–11] As the charge carriers in OFETs transport along a conducting channel, which is at the dielectric/organic semiconductor interface, a good dielectric is beneficial to the growth of the upper organic layer and can reduce the trap density at the dielectric/organic semiconductor interface. Therefore, by changing and modifying the gate dielectric, the performances of OFETs can be substantially improved.[8,12,13]

So far, various natural materials that are environmentally and biologically friendly, such as chicken albumen, silk fibroin (SF), and gelatin, have been reported to be used as the dielectrics in OFETs.[14–16] Those materials all serve as excellent gate dielectrics, which can enhance the crystal qualities of the semiconductors.[17] Meanwhile, with a high dielectric constant, those dielectric materials can reduce the operating voltages.[18,19] Besides, the SF is reported to be compatible with both p- and n-type organic semiconductors. The merits of the biocompatible dielectrics have great potential for a wide variety of applications, especially in the fields of bio-medicine and biosensors.

However, there are several remaining problems about the OFETs based on the SF dielectrics. First, a dry SF film is brittle and can be easily bent, so a robust SF dielectric is not easy to obtain;[20,21] second, the leakage current is relatively high in the SF based OFET, therefore leading to a low current on/off ratio and a high power consumption; third, there is few reports about the total resistance or contact resistance of the SF based OFET, so how the SF dielectric layers influence on the performance of the OFET needs to be further studied.

In this work, OFETs consisting of four different kinds of gate dielectrics poly(methyl methacrylate) (PMMA), SF, SF/PMMA, and PMMA/SF, which are biocompatible approved by U.S. Food and Drug Administration, are fabricated.[22,23] The electrical characteristics, such as mobility μ, the current on/off ratio, and threshold voltage V_T, of the devices with different gate dielectrics are discussed. And the total resistances, the contact resistances, and the interface trap densities of these devices are also investigated. By introducing a PMMA/SF bilayer dielectric, the grain size of pentacene is significantly increased and the leakage current is reduced, thus leading to a performance improvement of the OFETs.

2. Experiment

The structure of the OFET with different dielectric layers is shown in Fig. 1(a). The PMMA was dissolved in anisole with 10 wt.% concentration. An SF aqueous solution with ca. 6 wt.% concentration was extracted from cocoons of

*Project supported by the National Natural Science Foundation of China (Grant No. 61177032), the Foundation for Innovation Groups of the National Natural Science Foundation of China (Grant No. 61021061), the Fundamental Research Funds for the Central Universities, China (Grant No. ZYGX2010Z004), and the Scientific Research Staring Foundation for the Returned Overseas Chinese Scholars of the Education Ministry of China (Grant No. GGRYJJ08-05).

†Corresponding author. E-mail: jsyu@uestc.edu.cn

Chinese silkworm by following the extraction procedure with slight modifications.[20] Both PMMA and SF were spin-coated at 1500 rpm for 1 min and dried at 60 °C in an oven in air for 1 h. Then, 50 nm pentacene was thermally evaporated at a rate of 0.2 Å/s under 2×10^{-4} Pa. Subsequently, 50 nm Au electrodes were thermally evaporated using a metal shadow mask under 3×10^{-3} Pa. The electrical characteristics of the OFETs were measured using a Keithley 4200-SCS in air at room temperature. The morphologies of the PMMA and SF dielectric layers and the pentacene films grown on different dielectrics were characterized by atomic force microscopy (AFM). The dielectric constant of SF was analyzed with an HP4294A impedance analyzer by fabricating a capacitor of the metal–insulator–metal (MIM) configuration as shown in Fig. 1(b). The dielectric constant of SF is calculated to be ca. 6, which is consistent with the previous report.[21]

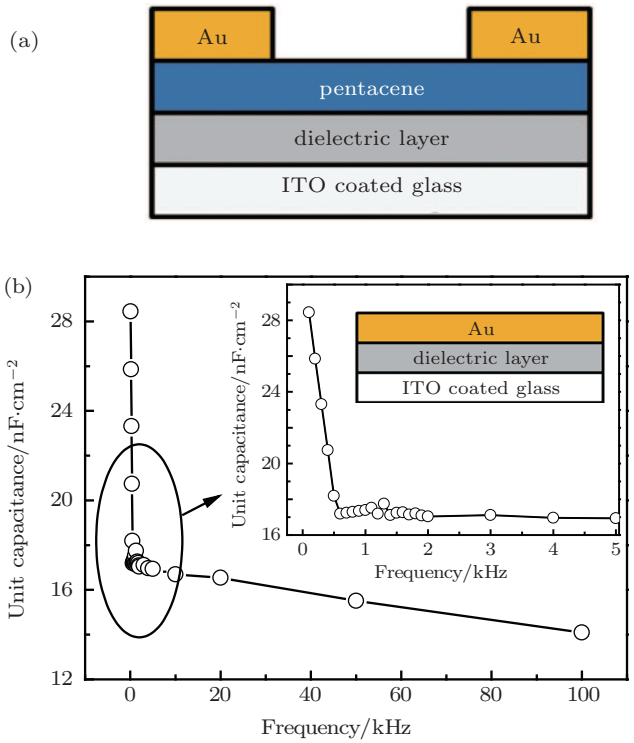

Fig. 1. (color online) (a) Device architecture of OFET in this study. (b) Capacitance versus frequency (*C*–*F*) for the MIM device. The inset shows the *C*–*F* in the frequency range of 0–5 kHz and the structure of the MIM device.

3. Results and discussion

Figure 2 shows the typical transfer and output curves of the four OFETs with different dielectric layers, i.e., with a PMMA dielectric layer (device A), an SF dielectric layer (device B), an SF/PMMA composite dielectric layer (device C), and a PMMA/SF bilayer dielectric layer (device D). The optimal performance is obtained in device D. The μ in the saturation regime is calculated from the transfer curves in Fig. 2 using the following equation:

$$I_{DS} = (W\mu C_i/2L)(V_{GS} - V_T)^2, \tag{1}$$

where I_{DS} is the drain current in the saturation regime, C_i is the capacitance per unit area, V_{GS} is the gate voltage, V_T is the threshold voltage, and W and L are the channel width and length, respectively. The charge mobilities of devices A, B, C, and D are 0.90 cm^2/V·s, 0.12 cm^2/V·s, 0.098 cm^2/V·s, and 0.21 cm^2/V·s, respectively. For detail, the values of μ, V_T, subthreshold slope, as well as current on/off ratio are listed in Table 1.

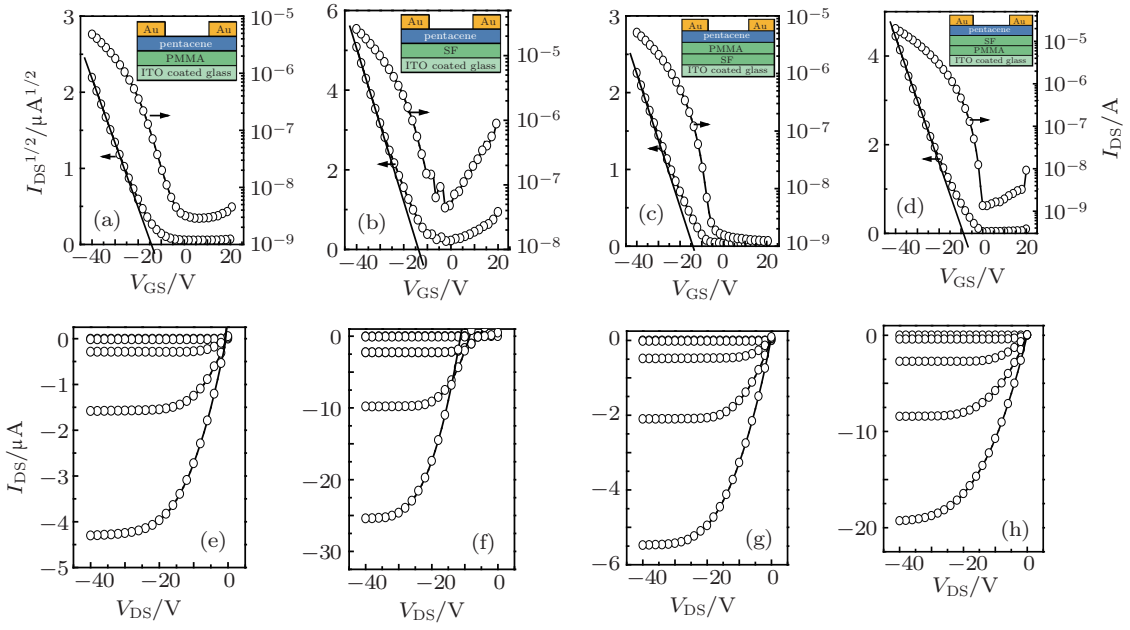

Fig. 2. (color online) Typical transfer and output characteristics of different devices: (a) and (e) device A, (b) and (f) device B, (c) and (g) device C, (d) and (h) device D. The channel width and length of the devices are 1 cm and 200 μm, respectively. The inset shows the specific structures of the OFETs with different dielectric layers.

Table 1. Field-effect mobility μ, threshold voltage V_T, subthreshold slope, and current on/off ratio of devices A, B, C, and D.

Device	μ/(cm^2/V·s)	V_T/V	Subthreshold slope/(V/dec)	On/off ratio /10^4
A	0.09	–15	6.5	0.2
B	0.12	–14	6.9	0.05
C	0.098	–14	3.9	0.41
D	0.21	–9	2.33	1.5

As shown in Fig. 2, the leakage currents are relatively high in devices A and B, which lead to low current on/off ratios. This could be ascribed to the relatively low insulating property of the single PMMA or SF dielectric layer compared to that of the bilayer dielectrics in devices C and D. The leakage current of device B is one order of magnitude higher than that of device A. The AFM images shown in Fig. 3(b) indicate that the SF dielectric layer has a smooth and homogeneous morphology. The root-mean square surface roughness value of the SF layer is 1.3 nm, which is a bit larger than that of the PMMA dielectric layer, which is 0.3 nm (Fig. 3(a)). The large roughness is mainly caused by the impurities in SF according to the AFM image. This could explain the high leakage current of device B shown in Fig. 2(b). On the other hand, regardless of the influence of the impurities, the roughness of the SF layer is similar to that of the PMMA dielectric layer.

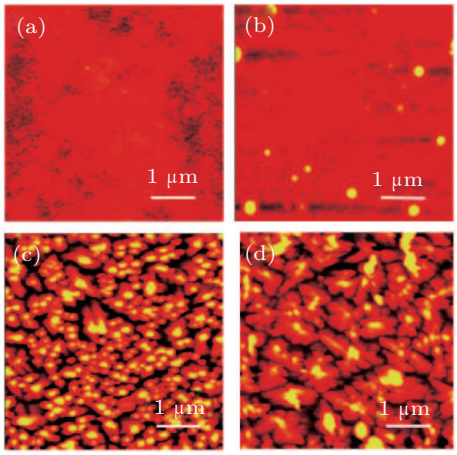

Fig. 3. (color online) AFM images of (a) PMMA dielectric layer, (b) SF dielectric layer, (c) pentacene grown on PMMA layer, and (d) pentacene grown on SF layer.

It is shown in Fig. 3 that the grain size of the pentacene crystal grown on the SF layer is much larger than that of the pentacene grown on the PMMA layer. The small crystal size of the pentacene film can introduce a high trap density into the device, thus leading to a degradation of the charge mobility. With a high degree of crystallinity and fewer grain boundaries, the performance of device D is enhanced. By introducing the PMMA/SF bilayer dielectric, the threshold voltage of device D is reduced to 9 V, which is about 60% lower than that of the other devices as listed in Table 1. Also, the current on/off ratio of device D increases almost three times compared with that of device C.

To further investigate the intrinsic cause for the performance improvement of the PMMA/SF OFET intuitively, the total resistance ($R_{\text{total}}W$) and the contact resistance (R_CW) are analyzed. The $R_{\text{total}}W$ and R_CW are calculated based on the transfer line method by using the following equation:[24,25]

$$R_{\text{total}} = R_C + \frac{L}{W\mu C_i(V_{GS} - V_T)}. \tag{2}$$

The R_{total} can be treated as a function of channel length L when W is a constant. As a result, R_CW can be extracted by giving $L = 0$ in Eq. (2). The $R_{\text{total}}W$ of the OFETs with various channel lengths of devices A, C, and D are calculated as shown in Fig. 4(a). It can be seen that the $R_{\text{total}}W$ of device D is the smallest, which is consistent with the device performance. Furthermore, it can also be seen that the R_CW of device D is also the smallest, which indicates a good organic/electrode contact of device D.

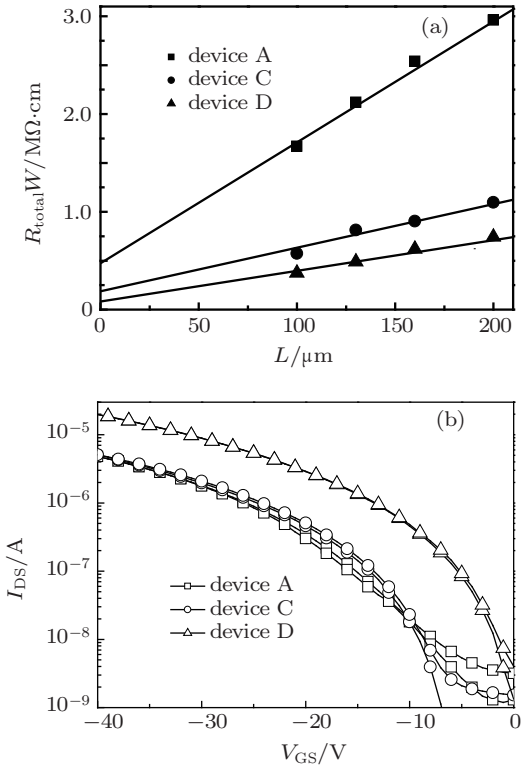

Fig. 4. (a) Total resistances and (b) I_{DS}–V_{GS} curves of devices A, C, and D.

Regardless of the inevitable imperfection of organic semiconductors, the charge carrier trap density N_{SS} is one of the causes for the channel resistance and the contact resistance.[26] To understand the contact resistance variation, we investigate the trap densities in devices A, C, and D. The total trap density of the OFETs can be determined by the following relation:[27]

$$N_{SS} = \left(\frac{S\log(e)}{k_BT/q} - 1\right)\frac{C_i}{q}, \tag{3}$$

where S is the subthreshold slope, q is the electronic charge, C_i is the capacitance per unit area, k_B is the Boltzmann's constant, and T is the absolute temperature. From Eq. (3),

we can figure out that the N_{SS} of devices A, C, and D are 2.26×10^{12} cm^{-2}·eV^{-1}, 1.67×10^{12} cm^{-2}·eV^{-1}, and 0.96×10^{12} cm^{-2}·eV^{-1}, respectively. This result is in accordance with the above study that the $R_C W$ of device D is the smallest.

From Fig. 4(b), it can be seen that there is a small hysteresis that appears in the I_{DS}–V_{GS} curves of devices A and C at V_{DS} of −40 V. This feature also indicates a larger N_{SS} of the PMMA/pentacene interface.[21] As is well known, the threshold voltage of an OFET is also strongly determined by the N_{SS} of the device.[28] The low N_{SS} value of device D serves as experimental evidence for the low threshold voltage of device D, and also for the formation of a good SF/pentacene interface, which indicates that the relatively rough SF layer does not affect the growth of the pentacene film. Therefore, by introducing the PMMA/SF composite dielectric layer, the dielectric/organic and the organic/electrode interfaces are both optimized.

4. Conclusion

In this paper, pentacene OFETs with various dielectric layers of PMMA and/or SF composites are fabricated and characterized. The results show that by using a PMMA/SF composite dielectric layer, the performance of the OFET, such as the threshold voltage and the current on/off ratio, can be greatly improved. The performance enhancement of the device is attributed mainly to the crystallization improvement of the pentacene film grown on the SF dielectric layer and the smaller interface trap density due to the adopting of the composite dielectric. The result also indicates that the composite dielectric layer is beneficial to the design of a novel architecture of OFETs with improved performance. Besides, the PMMA/SF composite dielectric layer is biocompatible, which shows a high potential to fabricate biocompatible electronic devices.

References

[1] Baude P F, Ender D A, Haase M A, Kelley T W, Muyres D V and Theiss S D 2003 *Appl. Phys. Lett.* **82** 3964

[2] Kelley T W, Baude P F, Gerlach C, Ender D E, Muyres D, Haase M A, Vogel D E and Theiss S D 2004 *Chem. Mater.* **16** 4413

[3] Forrest S R 2004 *Nature* **428** 911

[4] Gelinck G H, Huitema E A, van Veenendaal E, Cantatore E, Schrijnemakers L, Van Der Putten J B P H, Geuns T C T, Beenhakkers M, Giesbers J B, Huisman B H, Meijer E J, Benito E M, Touwslager F J, Marsman A W, VanRens B J E and Leeuw D M 2004 *Nature Mater.* **3** 106

[5] Yu J S, Yu X G, Zhang L and Zeng H J 2012 *Sens. Actuators B* **173** 133

[6] Zhao G, Cheng X M, Tian H J, Du B Q, Liang X Y and Wu F 2012 *Acta Phys. Sin.* **61** 218502 (in Chinese)

[7] Huang W, Yu J S, Yu X G, Li Y and Zeng H J 2012 *Thin Solid Films* **520** 6677

[8] DiBenedetto S A, Facchetti A, Ratner M A and Marks T J 2009 *Adv. Mater.* **21** 1407

[9] Sun Q J, Xu Z, Zhao S L, Zhang F J and Gao L Y 2011 *Chin. Phys. B* **20** 017306

[10] Zhou J L, Yu J S, Yu X G and Cai X Y 2012 *Chin. Phys. B* **21** 027305

[11] Shi W, Yu J S, Huang W, Yu X G and Zheng Y F 2013 *Appl. Phys. Lett.* **102** 111607

[12] Yoon M H, Yan H, Facchetti A and Marks T J 2005 *J. Am. Chem. Soc.* **127** 10388

[13] Shi W W, Li W, Yi M D, Xie L H, Wei W and Huang W 2012 *Acta Phys. Sin.* **61** 228502 (in Chinese)

[14] Chang J W, Wang C G and Huang C Y 2011 *Adv. Mater.* **23** 4077

[15] Tsai C L, Tsai L S and Hwang J C 2012 *Org. Electron.* **13** 3315

[16] Mao L K, Hwang J C and Chang T H 2013 *Org. Electron.* **14** 1170

[17] Capelli R, Amsden J J, Generali G, Toffanin S, Benfenati V, Muccini M, Kaplan D L, Omenetto F G and Zamboni R 2011 *Org. Electron.* **12** 1146

[18] Dimitrakopoulos C D, Purushothaman S, Kymissis J, Callegari A and Shaw J M 1999 *Science* **283** 822

[19] Dimitrakopoulos C D, Kymissis J, Purushothaman S, Neumayer D A, Duncombe P and Laibowitz R B 1999 *Adv. Mater.* **11** 1372

[20] Li M Z, Lu S Z, Wu Z Y, Tan K, Minoura N and Kuga S 2002 *Int. J. Biol. Macromol.* **30** 89

[21] Wang C H, Hsieh C Y and Hwang J C 2011 *Adv. Mater.* **23** 1630

[22] Kim D H, Kim Y S, Amsden J, Panilaitis B, Kaplan D L, Omenetto F G, Zakin M R and Rogers J A 2009 *Appl. Phys. Lett.* **95** 133701

[23] Hwang S W, Tao H, Kim D H, Cheng H, Song J K, Rill E, Brenckle M A, Panilaitis B, Won S M, Kim Y S, Song Y M, Yu K J, Ameen A, Li R, Su Y, Yang M, Kaplan D L, Zakin M R, Slepian M J, Huang Y G, Omenetto F G and Rogers J A 2012 *Science* **337** 1640

[24] Yu X G, Yu J S, Zhou J L, Huang J and Jiang Y D 2011 *Appl. Phys. Lett.* **99** 063306

[25] Yu X G, Yu J S, Huang W and Zeng H J 2012 *Chin. Phys. B* **21** 117307

[26] Liu C, Xu Y, Li Y, Scheideler W and Minari T 2013 *J. Phys. Chem. C* **117** 12337

[27] Narayanan U K N, Seignon S D and Nunzi J M 2005 *J. Phys. D: Appl. Phys.* **38** 1148

[28] Pernstich K P, Haas S, Oberhoff D, Goldmann C, Gundlach D J, Batlogg B, Rashida A N and Schitterb G 2004 *J. Appl. Phys.* **96** 6431